The Rise Ankle-Foot Orthosis Assists Dorsiflexion During Walking

Higher Device Stiffness Increases Ankle Dorsiflexion and Reduces Tibialis Anterior Activity in Healthy Participants

Pim B. Brouwer

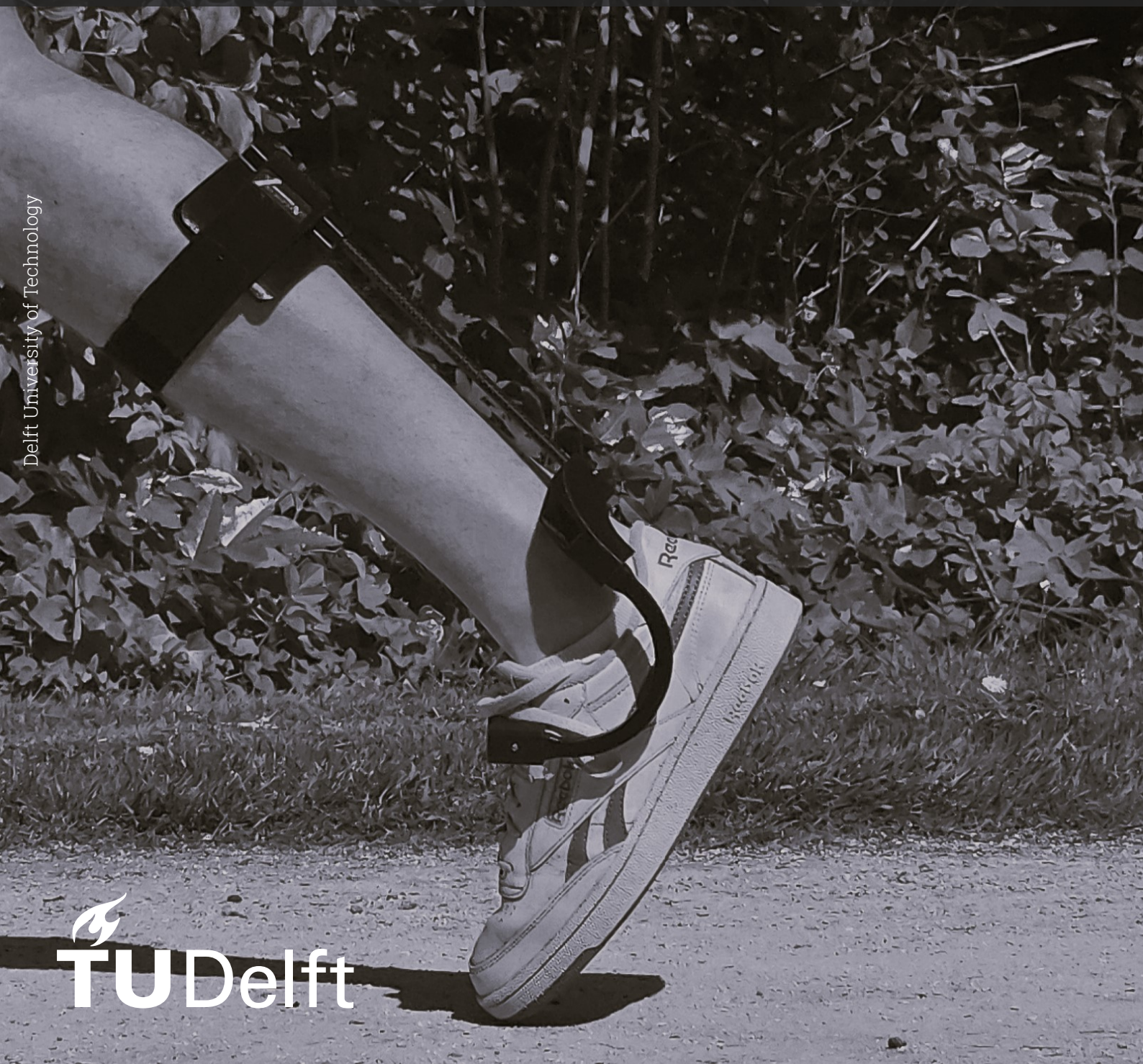

Delft University of Technology

TU Delft

The Rise Ankle-Foot Orthosis Assists Dorsiflexion During Walking

Higher Device Stiffness Increases Ankle Dorsiflexion and Reduces Tibialis Anterior Activity in Healthy Participants

by

Pim B. Brouwer

to obtain the degree of Master of Science

at the Delft University of Technology,

to be defended publicly on Friday June 6, 2025 at 09:30 AM.

Thesis committee:	dr. ir. W. Mugge
	ir. L.J. Zielstra
	dr. ir. E. van der Kruk
Project Duration:	November, 2024 - June, 2025
Faculty:	Faculty of Mechanical Engineering, Delft

An electronic version of this thesis is available at http://repository.tudelft.nl/.

TU Delft

ABSTRACT

Background: Foot drop is characterised by impaired active ankle dorsiflexion, affecting gait quality through foot slap during loading response and reduced toe clearance during swing phase. While ankle-foot orthoses (AFOs) are commonly prescribed, traditional designs often limit natural ankle motion during push-off and cause discomfort. There is a need for AFO designs that provide targeted dorsiflexion assistance while maintaining full plantarflexion mobility. The Rise AFO represents a novel approach, featuring complete ankle mobility and personalised dorsiflexion assistance determined by device stiffness.
Objective: To evaluate the effect of Rise AFO stiffness in reducing tibialis anterior activation and increasing ankle dorsiflexion during loading response and swing phase in healthy participants.
Methods: Ten healthy participants completed a randomised crossover trial comparing seven walking conditions on a treadmill at 4.4 km/h: baseline (no AFO), five Rise AFO stiffness configurations (0.05-0.39 Nm/deg), and a sham device with no stiffness. Primary outcomes included tibialis anterior EMG activity and ankle dorsiflexion. Secondary measures were plantarflexor activity, and sagittal plane knee and hip kinematics. Statistical parametric mapping analysed differences across the gait cycle.
Results: Compared to baseline, all Rise AFO configurations significantly reduced tibialis anterior activity during swing phase. The four stiffest configurations significantly increased swing phase ankle dorsiflexion, demonstrating a linear relationship between stiffness and mid-swing dorsiflexion (R^2 = 0.87). Loading response kinematics and muscle activity remained unchanged. Plantarflexor activity and proximal joint kinematics were not adversely affected. The sham device had no effect.
Conclusion: The Rise AFO effectively assisted dorsiflexion during swing phase while preserving natural plantarflexion, demonstrating potential as a personalised treatment for foot drop.

Keywords: *Ankle-foot orthosis, foot drop, biomechanical validation, 3D-printing, stiffness, gait, kinematics, surface electromyography, healthy participants*

1. Introduction

Foot drop, a condition characterised by impaired active ankle dorsiflexion, affects approximately 20% of stroke survivors and can significantly compromise gait and quality of life [1–5]. Figure 1 illustrates the standard phases and periods of normal gait [6], with the following two phases being particularly affected in individuals with foot drop. During the loading response, the forefoot may rapidly drop to the ground following heel strike due to insufficient eccentric control of the dorsiflexor muscles, a phenomenon known as foot slap [7]. In the swing phase, excessive plantarflexion can cause inadequate toe clearance, increasing the risk of stumbling or tripping [7]. To reduce the risk of tripping, individuals with foot drop often adopt compensatory strategies to improve foot clearance during swing phase. These strategies include increased knee and hip flexion, leg circumduction, hip hiking, and decreasing step length [5, 8–11]. While these adaptations allow functional gait, they also contribute to increased energy expenditure and may lead to secondary musculoskeletal problems over time [8, 12]. To improve gait by providing dorsiflexion assistance and preventing excessive plantarflexion of the ankle during the swing phase and loading response, an ankle-foot orthosis (AFO) is often prescribed [8, 9, 12, 13]. Most AFOs use a footplate that supports the plantar surface of the foot and attach to the calf or shin to keep the AFO secure on the lower leg, as shown in Figure 2A with a conventional off-the-shelf AFO.

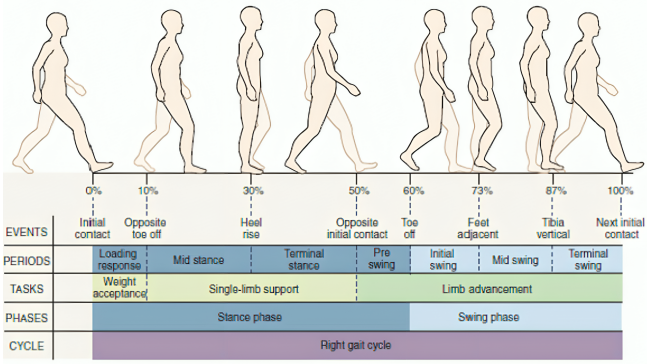

Figure 1: Illustration of the events and phases in normal gait [6]. With foot drop, the loading response and the swing phase are compromised.

The underlying causes of foot drop are diverse and include stroke, multiple sclerosis, central or peripheral nerve damage, and muscular disorders [2, 5, 11, 14]. Given the wide range of underlying pathologies that can lead to foot drop, no single AFO design is appropriate for all users. Instead, the choice of AFO is highly dependent on the individual's specific deficits in muscle function and gait mechanics [15]. For individuals with both dorsi- and plantarflexor weakness, as often seen in Charcot-Marie-Tooth disease or poliomyelitis [16], a rigid AFO provides necessary stability throughout the stance phase, though it can decrease plantarflexion power during push-off and reduce ankle mobility [17]. In cases of isolated dorsiflexor weakness, such as

those resulting from peroneal nerve injury, stance phase stability is typically less compromised since plantarflexor function remains intact. For these individuals, a less restrictive AFO design is preferred, as it provides sufficient dorsiflexion assistance during swing phase while preserving natural plantarflexor function during terminal stance and push-off [18].

While AFOs can improve gait in individuals with foot drop [8, 19], AFO use also comes with several limitations. AFO users with foot drop often mention that their AFO limits the range of motion during activities when ankle plantarflexion is desired, like walking down the stairs, riding a bike, or controlling the pedals in a car [20, 21]. Also, the stiff footplate of an AFO can cause discomfort due to pressure points or having limited space in the shoe, causing pain and blood circulation problems [21]. Thus, users mention that improved AFO design should balance between flexibility and stiffness, but that the exact solution differs for every individual [20].

Figure 2: Two AFOs that provide dorsiflexion assistance. **(A)** Conventional off-the-shelf AFO (SpryStep® Original, Thuasne, France) [13]. **(B)** Rise AFO (Rezolve Medical, Amsterdam, the Netherlands) [22]. Note that the Rise AFO should be placed between the tongue and the laces of the shoe, the foot shows the approximate position on the limb.

The Rise AFO (Rezolve Medical, Amsterdam, the Netherlands) [22], shown in Figure 2B, represents a novel approach to addressing these limitations and is the focus of this research. This 3D-printed AFO features a dorsal footplate positioned on top of the foot rather than beneath it. The goals of the Rise AFO are:

1. To personalise the dorsiflexion torque to the needs of each user, so that the foot is lifted in a neutral dorsiflexion position during the swing phase of gait and to control the descent of the foot during the loading response to prevent foot slap.
2. To maintain natural propulsive force during push-off by minimising resistance to ankle plantarflexion.
3. To increase comfort compared to traditional AFOs by eliminating the need for a stiff plantar-placed footplate.

To achieve these goals, the Rise AFO incorporates a compliant external bending strut that curves around the lateral malleolus and connects to the dorsally placed footplate. This design places the primary bending element outside the shoe, enabling easy customisation of stiffness to match individual needs. As shown in Figure 3, dorsiflexion assistance is provided through pre-tensioning: in its neutral state, the calf component sits anterior to the shank. When fitted, it is pulled posteriorly behind the calf, flexing the strut and generating a dorsiflexion moment at the ankle.

Figure 3: **(A)** Rise AFO when inserted in the shoe, shown in its neutral state with the calf component anterior to the shank. **(B)** Equipped Rise AFO after pre-tensioning. Parts of the Rise AFO: (1) footplate, (2) interchangeable stiffness modulator (external bending strut), (3) calf component.

The bending strut is intentionally designed as the most flexible section of the Rise AFO, functioning as the weakest link where the bending primarily occurs. By routing this strut around the lateral malleolus, the Rise AFO's rotational axis aligns with the anatomical ankle joint in the sagittal plane, preventing uncomfortable translation between the Rise AFO and lower leg during movement, which is not possible with a plantar footplate. Because the Rise AFO is 3D-printed, the stiffness of the bending strut can be customised by adjusting its thickness, enabling a personalised level of dorsiflexion assistance. However, the dorsal position of the footplate limits how stiff the Rise AFO can be made. During dorsiflexion, traditional AFOs with plantar footplates distribute force through the shoe sole, while the Rise AFO's dorsal placement applies pressure

directly onto the foot, potentially causing discomfort at higher stiffness levels. Based on these mechanical characteristics, traditional AFOs with high stiffness and plantar footplates are better suited for patients with substantial plantarflexor weakness or spasticity, providing the necessary stability during stance phase. In contrast, the Rise AFO is specifically intended for individuals with dorsiflexor weakness who retain adequate plantarflexor function.

An important aspect of AFO design for foot drop is the amount of dorsiflexion assistance provided, which is directly related to the device's bending stiffness [23]. The optimal level of support varies between individuals, depending on factors such as the degree of dorsiflexor weakness, the mass of the foot, and passive resistance from muscles and tendons [4, 15, 24]. As such, matching the mechanical response of the AFO to the user's specific needs is critical for improving gait. To facilitate this, the version of the Rise AFO used in this study was adapted to allow easy adjustment of its stiffness, by redesigning the external bending strut to be replaceable. This interchangeable component, referred to as the stiffness modulator, enables controlled variation in dorsiflexion torque across different configurations.

Investigating how different stiffness levels affect gait mechanics provides insight into how the Rise AFO can be tailored for optimal assistance. Therefore, the central research question addressed in this study is: What is the effect of varying the stiffness of the Rise AFO on lower leg muscle activity and sagittal plane kinematics during gait in healthy participants? The goal is to determine whether increased dorsiflexion support can reduce tibialis anterior activity during loading response and swing, without significantly increasing medial gastrocnemius and soleus activity during push-off. These effects can be assessed in healthy participants, enabling an initial evaluation of the AFO's function without burdening the clinical population. Because healthy participants are used, the kinematic analysis examines whether greater stiffness increases ankle dorsiflexion during loading response and swing phases while maintaining normal knee and hip movement patterns throughout the gait cycle. Muscle activity was recorded using surface electromyography (EMG), and joint kinematics were measured using a motion capture system.

2. Methods

2.1. AFO design

2.1.1. Parts and materials

The Rise AFO used in this research consists of three parts: a footplate, a calf component, and an interchangeable stiffness modulator that connects the two. These parts are shown and labelled in Figure 3. The footplate is 3D-printed in PLA and positioned between the tongue and laces of the shoe, serving as the interface that transmits dorsiflexion assistance to the foot. The stiffness modulator is a semi-circular arch with a radius of 45 mm and a 150° bend, 3D-printed in PLA using 100% concentric infill with the arch lying flat on the print bed to align the filament paths with the curvature of the part and maximise strength. The calf component consists of a carbon strut, a 3D-printed PLA calf plate with foam padding, and a Velcro band for fixation. All 3D-printed parts were fabricated using a Prusa MK3S printer (Prusa Research, Prague, Czech Republic).

2.1.2. AFO stiffness

The bending stiffness of the Rise AFO can be adjusted by replacing the interchangeable stiffness modulator with a stiffer or more compliant modulator. The interchangeable stiffness modulator functions mechanically as a curved beam with a trapezoidal cross-section (wider on the inner curvature) to reduce stress concentrations that occur during bending [25]. Five interchangeable stiffness modulators were developed with thicknesses ranging from 7.07 mm to 12.01 mm, corresponding to Rise AFO configurations C1 to C5, where C1 is the least stiff and C5 the stiffest. Technical drawings and detailed design rationale are provided in Appendix E.

Previous research has established that the tibialis anterior muscle generates approximately 0.42 Nm of torque to maintain the foot in a neutral position against gravity [26]. To replicate this physiological torque with the Rise AFO, a stiffness of 0.020 Nm/deg was targeted, accounting for the 21-degree flexion angle when the device is pre-tensioned. The third of the five modulators (median thickness) was designed to achieve this target stiffness value. The stiffness range for the other modulators was determined with preliminary testing during gait. The most compliant modulator was designed to provide minimal dorsiflexion assistance, while the stiffest modulator was selected to deliver substantial dorsiflexion support, though potentially at the cost of impeding plantarflexion during push-off.

To verify the mechanical performance of the designed modulators, all five configurations of the Rise AFO were tested for actual bending stiffness using the BRUCE stiffness tester, located at the Amsterdam UMC, The Netherlands [27]. The footplate of the Rise AFO was modified to be compatible with the BRUCE, and all measurements were performed by an experienced operator to improve reliability. The test setup is shown in Figure 4, and the corresponding anticipated and measured stiffness values are presented in Table 1.

2.2. AFO validation

2.2.1. Participants

Thirteen healthy participants (ages 21-28), consisting of eight males and five females, were recruited for the experiment. All participants had no self-reported motor or leg impairments and gave their informed consent prior to the experiment. The experiment was approved by the TU Delft ethics committee (approval number 5220).

2.2.2. Outcome measures

The aim of the Rise AFO is to prevent foot slap during the loading response and improve toe clearance during the swing phase, which are the two primary gait impairments in foot drop [7], while preserving natural plantarflexion during push-off. Therefore, the primary outcome measures in this randomised crossover trial are EMG activity of the tibialis anterior (the main ankle dorsiflexor) and ankle dorsiflexion angle during the loading response (0–10% of the gait cycle) and swing phase (60–100%). Secondary outcome measures included medial gastrocnemius and soleus EMG activity during stance (0–60% of the gait cycle) to evaluate whether the Rise AFO restricted plantarflexion during push-off. Sagittal plane knee and hip kinematics, along with contralateral limb kinematics, were assessed to analyse the effect of the Rise AFO on overall gait mechanics in healthy participants.

2.2.3. Procedures

Before data collection, participants were given 2 minutes to familiarise themselves with walking while wearing an AFO. Participants then walked on a treadmill at a normal walking speed of 4.4 km/h under seven conditions [28]. An overview of the experimental protocol is shown in Figure 5. The first baseline trial, lasting 2 minutes, was performed without an AFO (i.e., walking with standardised shoes only). Because previous research has shown that neuromuscular adaption to walking with an AFO takes time [29], the AFO trials were therefore extended to 5 minutes each. Thus, the baseline trial was followed by six randomised 5-minute trials: five using the Rise AFO with different stiffness values (0.05, 0.09, 0.19, 0.30, and 0.39 Nm/deg), and one using a sham AFO. The sham device used an interchangeable stiffness modulator with a thickness of 2 mm, resulting in an expected stiffness of 3.8×10^{-4} Nm/deg (less than 1% of the most compliant Rise AFO configuration), thus providing negligible dorsiflexion assistance. The order of these six trials was randomised using a Latin square design and is shown in Appendix A. Participants were unaware of the order in which the conditions were tested to ensure blinding. The AFO was worn on the left leg, and standardised shoes (shown in Appendix D) were used for all participants throughout the experiment. The experimental set-up is shown in Figure 6.

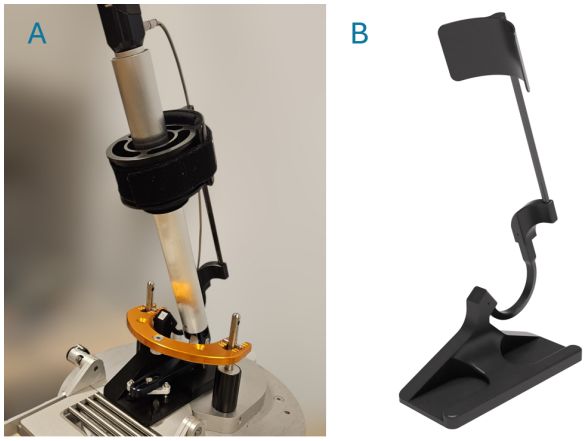

Figure 4: **(A)** AFO Stiffness measurement setup with the BRUCE [27]. **(B)** Render showing the adapted footplate to fit the Rise AFO in the BRUCE.

Table 1: AFO configurations with corresponding interchangeable stiffness modulator thickness, expected total AFO stiffness, and measured total AFO stiffness using the BRUCE stiffness tester. The sham AFO was too compliant to be measured with the BRUCE.

AFO configuration	Interchangeable stiffness modulator thickness (mm)	Expected total AFO stiffness (Nm/deg)	Measured total AFO stiffness (Nm/deg)
Configuration 1 (C1)	7.07	0.06	0.05
Configuration 2 (C2)	8.23	0.11	0.09
Configuration 3 (C3)	9.55	0.20	0.19
Configuration 4 (C4)	10.83	0.33	0.30
Configuration 5 (C5)	12.01	0.50	0.39
Sham AFO	2.00	3.8×10^{-4}	N/A

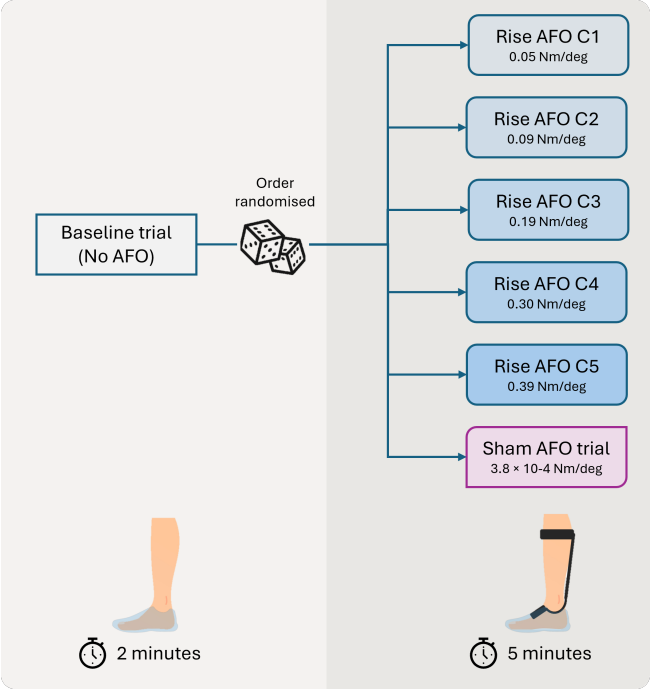

Figure 5: Experimental protocol overview. Participants completed a 2-minute baseline trial without an AFO, followed by six randomised 5-minute trials: five with the Rise AFO at increasing stiffness levels (C1-C5: 0.05-0.39 Nm/deg) and one with a sham AFO (3.8×10^{-4} Nm/deg). All trials were conducted at a standardised walking speed of 4.4 km/h on a treadmill.

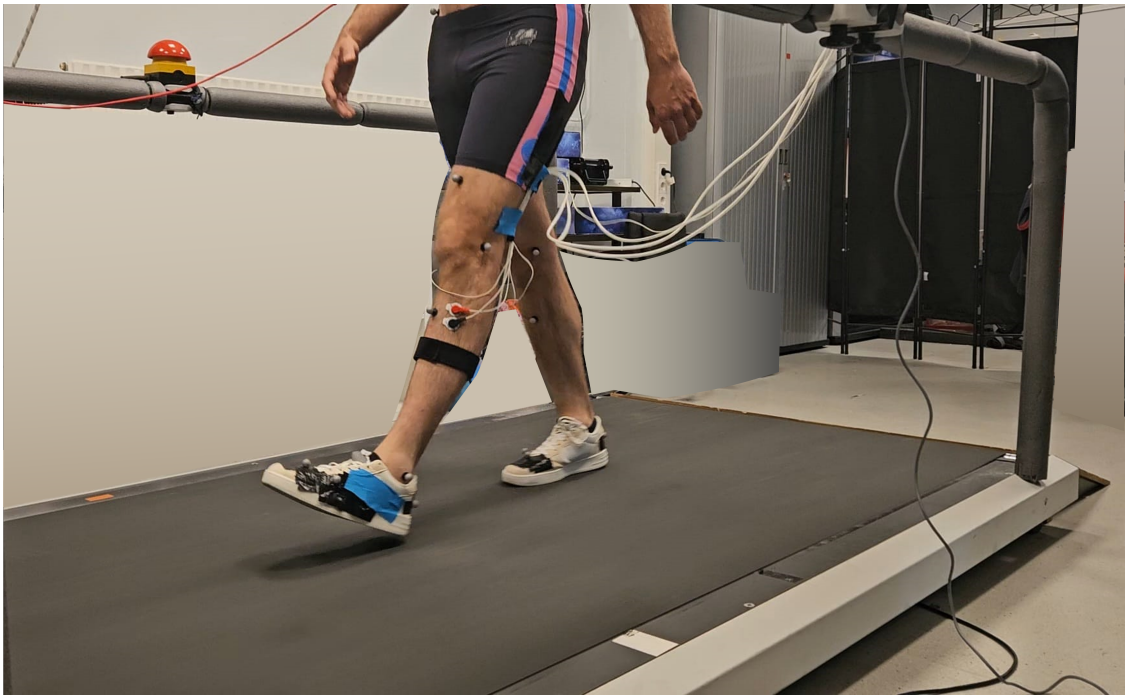

Figure 6: Experiment set-up featuring the treadmill with emergency stop, EMG electrodes, standardised shoes, and motion capture markers used.

2.2.4. EMG

Muscle activity of the lower left leg was captured at 2048 Hz using a bipolar EMG system (TMSi Porti, Oldenzaal, the Netherlands). Electrodes were placed on the tibialis anterior, medial gastrocnemius and soleus muscles with an inter-electrode distance of 20 mm. Electrode placement was performed according to the SENIAM European Recommendations for Surface ElectroMyoGraphy [30]. The raw EMG signal was bandpass filtered (20–500 Hz, zero-phase 4th order Butterworth) and then processed using a root-mean-square algorithm (100 ms moving window) [31].

To allow comparison of muscle activity across participants and conditions, normalisation of the EMG signals was necessary. Two main approaches are commonly employed: normalisation to maximal voluntary isometric contraction (MVIC) values, or dynamic peak normalisation [32]. MVIC normalisation is generally preferred, as it relates EMG activity to the individual's maximal muscle activation capacity. However, dynamic peak normalisation, which normalises EMG to the peak dynamic activity observed during functional tasks, can be used when MVIC testing is unreliable or inconsistent [33]. Before the walking trials, all participants performed three five-second MVIC trials for both dorsiflexion and plantarflexion to establish maximum reference values [31]. During these trials, force output was measured using a digital scale to capture maximal effort, the positions used during these trials are shown in Appendix B. The acquired MVIC values were used as the primary reference for EMG normalisation. When MVIC recordings proved unreliable across participants, dynamic peak normalisation based on baseline walking data was employed as an alternative for all participants [33]. To reduce the risk of normalising to outliers, a moving average filter with a window size of 0.1 seconds was applied prior to identifying the peak value.

2.2.5. Kinematics

Motion capture was performed with a marker-based motion capture system (Qualisys AB, Gothenburg, Sweden), consisting of six wall-mounted Oqus cameras and two tripod-mounted Miqus cameras. Motion capture data was collected using Qualisys Track Manager and recorded at 200 Hz. Markers were placed on the body according to the Qualisys Sports Marker Set, from which only the markers on the lower body were used, Appendix C shows the exact locations of the markers. Foot markers were placed on the shoe instead, as shown in Appendix D, since the Rise AFO requires a shoe to function properly. Marker trajectories were automatically identified using a pre-trained AIM (Automatic Identification of Markers) model. Marker identification was manually checked, after which Qualisys Track Manager was used to solve the skeleton calculations corresponding to the marker positions. The skeleton calculations resulted in joint position and angles for the ankle, knee and hip joints, and the segments connecting these joints. Marker and skeleton data was then exported to MATLAB (The Mathworks, Natick, USA) for further analysis.

2.2.6. Data analysis

The sagittal plane kinematics were extracted from the motion capture data for the left and right ankle, knee, and hip joints. Normalised EMG and kinematic signals were segmented into individual steps, and the last 94 steps from each measurement were retained to ensure equal data length across participants. This number corresponded to the lowest step count recorded during the two-minute baseline condition. All steps were time-normalised to the gait cycle (0–100%) to account for variability in gait speed and stride duration. For each participant and condition, signals were averaged across steps to obtain a single representative gait cycle.

One-dimensional statistical parametric mapping (SPM) [34] was used to analyse EMG activity and kinematics across the gait cycle. The alpha level was set to 0.05. Prior to SPM analysis, data normality was assessed using the D'Agostino–Pearson K^2 test [35]. When normality was violated, non-parametric testing was employed. A repeated measures ANOVA was then performed to test for differences across stiffness conditions. If significant differences were found, post-hoc pairwise comparisons were conducted using paired t-tests. A Bonferroni correction was applied to control the family-wise error rate. The average effect sizes within the significant regions identified in the post-hoc comparisons were calculated using Cohen's *d* to quantify the magnitude of the differences between conditions.

3. Results

Thirteen participants were recruited for the experiment; of which three were excluded from analysis due to EMG signal artifacts. Table 2 presents the characteristics of the ten included participants.

Table 2: Included participant characteristics

Characteristics (N=10)	Mean ± SD
Age (years)	24.2 ± 1.5
Sex	6 male, 4 female
Height (cm)	182.0 ± 9.5
Weight (kg)	71.3 ± 8.7
Shoe size (EU)	42.0 ± 2.7

3.1. EMG

The maximum EMG values recorded during the MVICs were found to be unreliable for normalisation, as many participants exhibited greater EMG activity during walking than during MVIC testing. Therefore, the raw EMG signals were normalised to the peak dynamic EMG value recorded during the baseline walking trial. K^2 testing showed that EMG data for all muscles were not normally distributed. Consequently, SPM with non-parametric testing was employed for statistical analysis of the EMG data.

3.1.1. Tibialis anterior

As expected, tibialis anterior activity was decreased by walking with the Rise AFO ($p < 0.001$). The post-hoc pairwise comparisons between the baseline condition and all other conditions are shown in Figure 7 (all comparisons shown in Appendix F). Tibialis anterior activity during terminal swing (85–99% gait cycle) was significantly reduced compared to baseline in all Rise AFO configurations ($p < 0.001$), with effect sizes ranging from $d = 2.04$ (C1) to $d = 2.45$ (C3). As anticipated, no difference was found between walking with the sham device and the baseline condition, while C2, C4, and C5 all showed a decrease in tibialis anterior activity in the terminal swing phase compared to the sham AFO (all $p < 0.001$, respective d: 2.16, 2.07, 2.01). While a negative trend between AFO stiffness and tibialis anterior activity was observed during the loading response (0–10% of gait cycle), no significant decrease in muscle activity was found during this phase.

3.1.2. Medial gastrocnemius

A significant effect was found with SPM repeated measures ANOVA for medial gastrocnemius activity ($p < 0.001$). The results for pairwise comparison of medial gastrocnemius activity for all combinations are shown in Appendix G. Surprisingly, post-hoc analysis revealed a reduction in medial gastrocnemius activity during mid-stance (20 – 26% of the gait cycle) compared to baseline measurements for the C1 and C4 Rise AFO configurations (C1, C4; both $p < 0.001$; respective d: 2.17 and 1.73). No significant differences were found between the Rise AFO configurations or between the sham and any condition.

3.1.3. Soleus

A significant difference across all conditions was found for soleus activity ($p < 0.001$). Appendix H shows all post-hoc comparisons for soleus activity. An unexpected reduction was found in muscle activity from the baseline to the C2 condition ($p < 0.01$, $d = 1.69$) in the terminal swing phase (95–96% of the gait cycle). Stance phase soleus activity also showed an unexpected decreasing trend across all conditions and the sham AFO compared to baseline, although this was not statistically significant.

3.2. Kinematics

3.2.1. Ankle dorsiflexion

Sagittal plane ankle kinematics were normally distributed. SPM repeated measures ANOVA revealed significant effects ($p < 0.001$) of walking with the Rise AFO on ankle dorsiflexion. Post-hoc analyses indicated

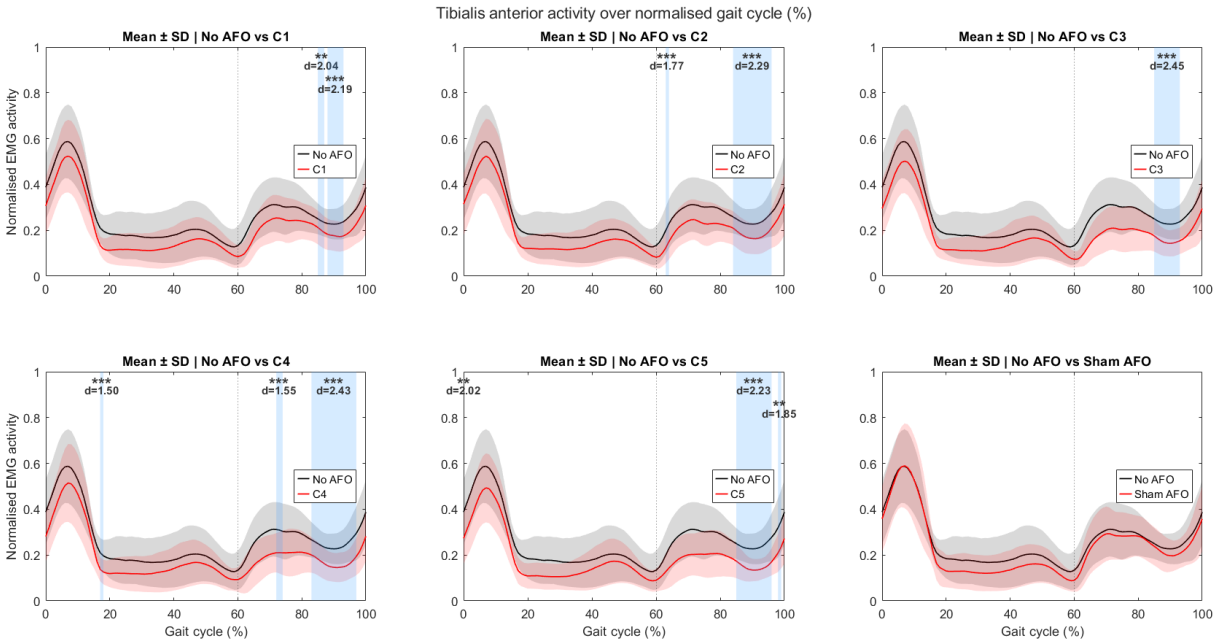

Figure 7: Average normalised tibialis anterior EMG activity across all participants over the gait cycle, with standard deviation represented by shaded areas. Each subplot shows a comparison between the baseline condition (no AFO) and one of the Rise AFO configurations (C1–C5) or the sham AFO. Statistically significant differences identified by SPM are highlighted in blue, with significance levels indicated (*$p \leq 0.05$, **$p \leq 0.01$, ***$p \leq 0.001$) and corresponding effect sizes (Cohen's d) shown above. The x-axis denotes the normalised gait cycle (0–100%), and the y-axis normalised muscle activity. The vertical line at 60% marks the transition from stance to swing phase.

multiple significant differences between configurations. All differences were found during the swing phase, with most occurring between toe-off and mid-swing. Figure 8 presents the comparisons for average ankle joint dorsiflexion over the gait cycle between the baseline condition without AFO and all other conditions. Appendix I shows figures for all pairwise post-hoc ankle dorsiflexion comparisons. No differences were found between the baseline condition and the sham AFO, indicating that ankle kinematics were similar for both conditions. Similarly, no difference was found between the baseline condition and the least stiff configuration of the Rise AFO (C1). Compared to the baseline condition, an increase in ankle dorsiflexion was found for the stiffer AFO configurations (C2, C3, C4, and C5; all $p < 0.001$). Effect size was smallest for C2 ($d = 2.50$) and largest for C4 ($d = 3.16$). No differences were found during the loading response for ankle kinematics between any of the conditions.

Compared to the sham condition, C1 showed a brief increase in ankle dorsiflexion immediately after toe-off ($p < 0.01$, $d = 2.17$), whereas C3, C4, and C5 showed a sustained increase (all $p < 0.001$, respective d: 2.24, 2.70, 3.12) lasting from toe-off until mid-swing.

Post-hoc comparisons between stiffness configurations for the Rise AFO showed an increase in ankle dorsiflexion during the swing phase between the least stiff configuration (C1) and the two stiffest configurations (C4, C5; both $p < 0.001$; both $d > 2.30$). The second stiffest configuration (C4) also showed an increase in ankle dorsiflexion compared to the second most compliant configuration (C2), just before heel strike ($p < 0.001$, $d = 2.46$).

Given that adequate dorsiflexion during mid-swing (73–87% of the gait cycle) is critical for toe clearance [36], a linear regression analysis was performed to quantify the relationship between total AFO stiffness and average ankle flexion during the mid-swing phase. The analysis revealed a linear relationship ($R^2 = 0.87$, $p = 0.006$), as shown in Figure 9. The regression equation was:

$$\theta = 14.60k - 3.92 \quad (1)$$

where θ is ankle flexion angle (deg) and k is AFO stiffness (Nm/deg).

3.2.2. Knee flexion

Sagittal plane knee kinematics data were not normally distributed, thus non-parametric testing was employed. Knee flexion patterns were also affected by the Rise AFO configuration, as indicated by a significant effect in the SPM repeated measures ANOVA ($p < 0.01$). However, post-hoc analysis revealed less pronounced effects than those observed at the ankle joint. A significant decrease in knee flexion was detected from the lowest stiffness (C1) to the highest stiffness (C5) configurations for a short time during initial swing (66–67% of the gait cycle, $p < 0.01$, $d = 2.07$).

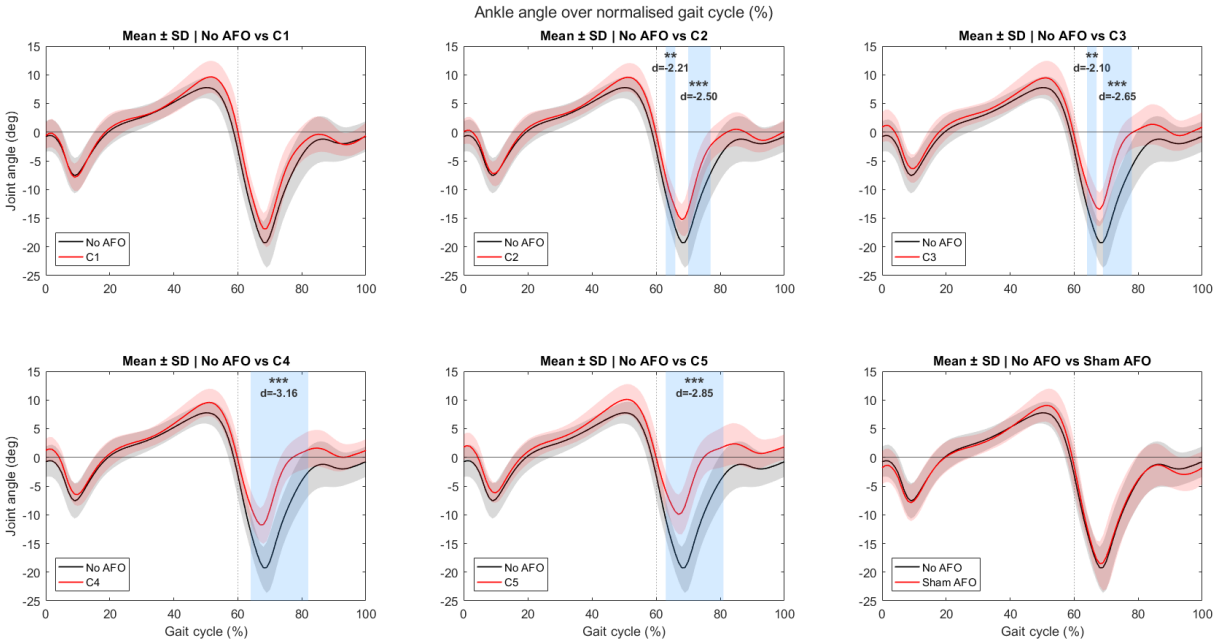

Figure 8: Average ankle flexion angle across all participants over the gait cycle, with standard deviation represented by shaded areas. Each subplot shows a comparison between the baseline condition (no AFO) and one of the Rise AFO configurations (C1–C5) or the sham AFO. Statistically significant differences identified by SPM are highlighted in blue, with significance levels indicated (*$p \leq 0.05$, **$p \leq 0.01$, ***$p \leq 0.001$) and corresponding effect sizes (Cohen's d) shown above. The x-axis denotes the normalised gait cycle (0–100%), and the y-axis the ankle flexion angle, where dorsiflexion is defined as positive and plantarflexion as negative. The vertical line at 60% marks the transition from stance to swing phase.

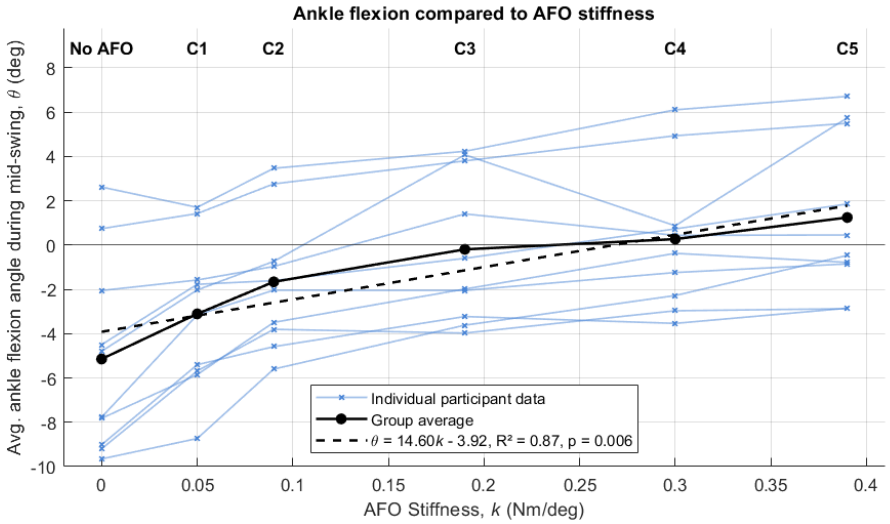

Figure 9: Regression analysis between average ankle flexion angle during the mid-swing period and AFO stiffness. Data of each participant is shown in blue, while the group average and regression analysis are shown in black. The x-axis represents the total AFO stiffness for every condition, while the y-axis represents the average ankle flexion angle during the mid-swing period (73–87 % of the gait cycle), dorsiflexion is defined as positive and plantarflexion is defined as negative. No AFO is the baseline condition without AFO, while C1 to C5 are configurations of the Rise AFO with increasing stiffness

3.2.3. Hip flexion

Sagittal plane hip kinematics data were not normally distributed, thus non-parametric testing was employed. SPM repeated measures ANOVA analysis revealed a significant effect of AFO configuration on hip flexion ($p < 0.01$). Appendix K shows all post-hoc comparisons, where no significant pairwise differences were identified.

3.3. Non AFO leg

The AFO was worn on the left leg for all participants. Group-level analysis of the right leg revealed no significant differences in ankle, knee, or hip flexion. EMG activity was not measured for the right leg.

4. Discussion

4.1. EMG

Walking with the Rise AFO consistently reduced tibialis anterior muscle activation in the swing phase compared to walking without an AFO. Importantly, this effect was observed across all five stiffness configurations of the Rise AFO but was not present with the sham AFO. This pattern indicates that the reduced tibialis anterior activity resulted from the dorsiflexion assistance provided by the AFO's stiffness properties, rather than the weight or presence of the device itself. This is further supported by significant decreases in tibialis anterior activity between the sham condition and configurations C2, C4, and C5. Although statistical analysis did not reveal significant differences in tibialis anterior recruitment between the various stiffness configurations, effect size compared to the baseline condition was larger for stiffer configurations, showing that the reduction in tibialis anterior was larger with increased stiffness. A negative trend for tibialis anterior activity during the loading response was observed but did not reach significance, possibly due to high inter-participant variability in EMG activity during this gait phase.

The Rise AFO showed minimal effects on plantarflexor muscle activity. Crucially, none of the configurations increased plantarflexor activity, indicating that the Rise AFO does not substantially impede plantarflexion. Had the device created meaningful resistance to plantarflexion, an increase in calf muscle activity would have been expected in response. This can be explained by the biomechanical properties of these muscle groups, as the ankle plantarflexors are 3-4 times stronger than the ankle dorsiflexors [37] and are therefore potentially less affected by the relatively small resistance provided by the Rise AFO. Contrary to expectations, all configurations appeared to reduce medial gastrocnemius and soleus activity during stance phase compared to baseline, although only the medial gastrocnemius reductions for configurations C1 and C4 briefly reached statistical significance. These two observed reductions in plantarflexor activity were unexpected and may be explained by decreased EMG signal quality over time due to electrode gel drying or loosening from perspiration and movement. Since baseline measurements were always conducted first, electrode contact quality may have been optimal during these initial recordings compared to subsequent conditions. This systematic timing difference could therefore have contributed to the apparent reductions in muscle activity across all AFO conditions. To mitigate this in future studies, baseline measurements should be randomised with other conditions, and recording durations should remain consistent across all conditions.

A limitation for the analysis of EMG data was the normalisation method employed in this study. The intended method was normalisation to maximum voluntary isometric contractions (MVIC) [33]. However, to facilitate force measurements using a digital scale in a simple and practical setup, the joint and body positions for the MVIC tests were modified from those recommended in the literature [31, 38], which likely compromised maximal muscle activation. Several participants consistently exhibited greater EMG activity during walking than during MVIC trials, resulting in substantial inter-participant variance. Therefore, dynamic peak normalisation was used instead [33]. This alternative approach reduced variance between participants and allowed for more reliable comparisons across AFO conditions. However, a key limitation is that it does not permit quantification of absolute muscle activation levels, limiting analysis to relative comparisons between conditions.

Despite employing peak dynamic normalisation, substantial variance remained between participants. This variability, combined with the limited sample size of ten participants, significantly reduced this study's statistical power. The strict Bonferroni correction applied to post-hoc comparisons increased the risk of Type II errors, potentially masking real effects of the Rise AFO on muscle activation patterns. The large effect sizes found in statistically significant regions should be interpreted with caution given these limitations. With small samples, significance testing naturally tends to detect only substantial differences between conditions. This means more subtle but clinically relevant effects might have been missed, while the magnitude of detected effects could be somewhat exaggerated. This creates a situation where only large effects reach statistical significance, yet these same large effects must be viewed cautiously because of potential estimation bias in small samples [39]. Future research would benefit from larger participant groups to improve statistical power, better MVIC testing protocols to reduce variability, and possibly more balanced

statistical approaches that manage both Type I and Type II error risks. These improvements would allow for better understanding of muscle activation patterns across Rise AFO configurations, including detection of smaller but potentially important clinical effects and more accurate estimation of effect sizes.

4.2. Kinematics

The Rise AFO demonstrated significant effects on ankle kinematics. Although the study was conducted on healthy participants who do not require dorsiflexion assistance, an increase in ankle dorsiflexion was observed across the four stiffest configurations. A strong correlation was found between AFO stiffness and average ankle dorsiflexion during mid-swing (R^2 = 0.87), indicating that increased stiffness consistently led to greater dorsiflexion.

SPM analysis showed that dorsiflexion increased between toe-off and mid-swing, the phase where toe clearance is essential for individuals with foot drop. This aligns with the function of the interchangeable stiffness modulator, which acts as a spring and generates its peak dorsiflexion torque just after toe-off, when the ankle is maximally plantarflexed.

In contrast, the effect of the Rise AFO on knee and hip flexion was minimal. While a statistically significant decrease in knee flexion was detected between the lowest and highest stiffness configurations, this occurred only briefly during initial swing (66–67% of gait cycle) and is unlikely to be clinically meaningful due to the short duration of the effect. This limited effect on proximal joints is likely due to the use of healthy participants, who do not require compensatory strategies to achieve toe clearance. In individuals with foot drop, increased knee and hip flexion are common compensatory mechanisms [8, 9, 40]. However, such adaptations were unnecessary in this population, and therefore the Rise AFO exerted limited influence on these joints. Similarly, the lack of difference in ankle kinematics during the loading response likely stems from the absence of foot slap pathology in healthy participants, a condition the Rise AFO is designed to address but was not present to correct in this study population.

4.3. AFO stiffness

As the Rise AFO attaches to the top of the foot rather than using a traditional footplate beneath the foot, the footplate had to be modified to enable compatibility with the BRUCE stiffness testing device. Because the modified footplate for the BRUCE was stiffer than the footplate of the Rise AFO, the stiffness values obtained using the BRUCE may differ slightly from the actual stiffness of the Rise AFO configurations employed in this study.

For the more compliant configurations (C1–C3), the measured stiffness values closely matched the expected results. However, for the two stiffer configurations, measured stiffness was lower than anticipated. The expected stiffness was calculated based on the dimensions of the interchangeable stiffness modulator, which is the most compliant component and therefore primarily responsible for the overall AFO stiffness. In the stiffer configurations, however, deformation was not restricted to the stiffness modulator alone and other components of the AFO also deformed. This led to a reduction in measured stiffness compared to the expected values: a decrease of 9% for C4 and 22% for C5.

Bending of the external stiffness modulator may have caused misalignment between the bending axes of the Rise AFO and the ankle joint, particularly in the stiffer configurations where bending also occurred in other components. This misalignment could lead to unwanted translation at the attachment point to the leg, resulting in discomfort and the need for readjustment.

4.4. Relevance and future direction

This study demonstrated that the Rise AFO successfully assists ankle dorsiflexion in healthy participants, as evidenced by reduced tibialis anterior activity and increased dorsiflexion during swing phase. These findings align with the device's intended purpose for individuals with foot drop. However, several limitations highlight the need for further validation in the target population. First, the study was conducted in healthy participants who do not experience foot drop pathology, limiting assessment of clinically relevant outcomes such as foot slap correction during loading response. Second, optimal stiffness personalisation could not be evaluated since healthy individuals do not require dorsiflexion correction. Building on these promising preliminary findings, future research should focus on clinical validation in individuals with foot drop to assess the Rise AFO's effectiveness in addressing both swing phase toe clearance and loading response foot slap, including longitudinal studies to evaluate long-term outcomes such as durability, user satisfaction, functional improvements over time, and any potential complications or adaptations. Additionally, investigating individualised stiffness optimisation will be crucial to determine the appropriate level of assistance that restores adequate ankle dorsiflexion without compromising plantarflexion function. A combination of kinematic analysis of all lower limb joints with kinetic measurements such as push-off power generation and energy expenditure could provide valuable insights for personalising stiffness settings and optimising gait efficiency in foot drop patients [15].

5. Conclusion

This study provides the first biomechanical validation of a novel 3D-printed dorsal-footplate AFO design in healthy individuals. The Rise AFO successfully reduced tibialis anterior activity during swing phase across all stiffness configurations, with large effect sizes (d = 2.19–2.45). Furthermore, ankle dorsiflexion increased linearly with device stiffness (R^2 = 0.87), demonstrating that assistance levels can be precisely modulated through mechanical design. Tibialis anterior activity during the loading response was not significantly reduced. To assess whether the Rise AFO can assist with foot slap in the loading response, further evaluation in individuals with foot drop is necessary. While changes in plantarflexor activity were observed, their interpretation was limited by a small sample size and potential reduced EMG signal quality over time. Overall, these findings suggest that the Rise AFO can assist dorsiflexion during swing and supports improved toe clearance while preserving natural plantarflexion during push-off. The systematic relationship between stiffness and ankle dorsiflexion indicates potential for personalised stiffness tuning. Future studies in individuals with foot drop are essential to evaluate clinical benefits, determine optimal stiffness levels, and assess long-term outcomes of the Rise AFO.

6. Acknowledgements

I would like to express my sincere gratitude to my supervisors, Dr.ir. Winfred Mugge and ir. Lennart Zielstra. Lennart, your endless enthusiasm and practical insight made a significant difference during the often challenging period known as graduating from a TU Delft master. Your support helped me navigate the process more smoothly and with greater confidence. Winfred, your academic expertise and sharp critical feedback consistently pushed the quality of my work to a higher level, a standard I could not have reached on my own.

My sincere thanks to everyone at Rezolve Medical for making this assignment possible and for the endless games of ping-pong we played to keep the ideas and energy going. Special thanks go to the Amsterdam UMC, and particularly Niels Waterval for his expertise, time, and for providing access to the BRUCE AFO stiffness testing device, which contributed significantly to this research. I am also grateful to my fellow students at the NMC lab for the many insightful discussions and for generously participating in my experiment.

And a final thanks to my friends, family, and housemates, for all the good times in between the studying that made this past year an enjoyable one. And lastly, I want to thank Tinka, for always having my back and being there for me this year and all those to come.

References

[1] K. Sota, Y. Uchiyama, M. Ochi, S. Matsumoto, K. Hachisuka, and K. Domen, “Examination of Factors Related to the Effect of Improving Gait Speed With Functional Electrical Stimulation Intervention for Stroke Patients,” *PM&R*, vol. 10, no. 8, pp. 798–805, Aug. 2018.

[2] F. Amitrano, A. Coccia, G. Cesarelli, *et al.*, “The impact of ankle-foot orthosis on walking features of drop foot patients,” in *2022 IEEE International Workshop on Metrology for Extended Reality, Artificial Intelligence and Neural Engineering, MetroXRAINE 2022 - Proceedings*, pp. 87–92.

[3] L. Zollo, N. Zaccheddu, A. L. Ciancio, *et al.*, “Comparative analysis and quantitative evaluation of ankle-foot orthoses for foot drop in chronic hemiparetic patients,” *European Journal of Physical and Rehabilitation Medicine*, vol. 51, no. 2, pp. 185–196, 2015.

[4] N. B. Bolus, C. N. Teague, O. T. Inan, and G. F. Kogler, “Instrumented Ankle–Foot Orthosis: Toward a Clinical Assessment Tool for Patient-Specific Optimization of Orthotic Ankle Stiffness,” *IEEE/ASME Transactions on Mechatronics*, vol. 22, no. 6, pp. 2492–2501, Dec. 2017.

[5] M. Błażkiewicz, I. Wiszomirska, K. Kaczmarczyk, G. Brzuszkiewicz-Kuźmicka, and A. Wit, “Mechanisms of compensation in the gait of patients with drop foot,” *Clinical Biomechanics*, vol. 42, pp. 14–19, Feb. 2017.

[6] R. Di Gregorio and L. Vocenas, “Identification of Gait-Cycle Phases for Prosthesis Control,” en, *Biomimetics*, vol. 6, no. 2, p. 22, Jun. 2021.

[7] M. Alam, I. A. Choudhury, and A. B. Mamat, “Mechanism and Design Analysis of Articulated Ankle Foot Orthoses for Drop-Foot,” en, *The Scientific World Journal*, vol. 2014, no. 1, p. 867 869, 2014.

[8] P. Caravaggi, G. Rogati, L. Zamagni, *et al.*, “Functional evaluation of a novel fibreglass-reinforced polyamide custom dynamic AFO for foot drop patients: A pilot study,” *Gait and Posture*, vol. 109, pp. 41–48, 2024.

[9] C. D. M. Nikamp, J. van der Palen, H. J. Hermens, J. S. Rietman, and J. H. Buurke, “The influence of early or delayed provision of ankle-foot orthoses on pelvis, hip and knee kinematics in patients with sub-acute stroke: A randomized controlled trial,” *Gait and Posture*, vol. 63, pp. 260–267, 2018.

[10] E. Pourhoseingholi and N. Tafti, “The Immediate Effect of the Novel Hybrid Passive Spring Damper Ankle-Foot Orthosis on Spatiotemporal Parameters of Walking in Patients with Multiple Sclerosis,” *Journal of Prosthetics and Orthotics*, 2024.

[11] A. I. Kottink, L. J. Oostendorp, J. H. Buurke, A. V. Nene, H. J. Hermens, and M. J. IJzerman, “The Orthotic Effect of Functional Electrical Stimulation on the Improvement of Walking in Stroke Patients with a Dropped Foot: A Systematic Review,” en, *Artificial Organs*, vol. 28, no. 6, pp. 577–586, 2004.

[12] A. I. R. Kottink, M. J. B. Tenniglo, W. H. K. De Vries, H. J. Hermens, and J. H. Buurke, “Effects of an implantable two-chanel peroneal nerve stimulator versus conventional walking device on spatiote mporal para meters and kine matics of hemiparetic gait,” *Journal of Rehabilitation Medicine*, vol. 44, no. 1, pp. 51–57, 2012.

[13] D. Rimaud, R. Testa, G. Y. Millet, and P. Calmels, “Effects of carbon versus plastic ankle-foot orthoses on gait outcomes and energy cost in patients with chronic stroke,” *Journal of Rehabilitation Medicine*, vol. 56, 2024.

[14] R. K. Nath and C. Somasundaram, “Incidence, Etiology, and Risk Factors Associated with Foot Drop,” *Eplasty*, vol. 23, e16, Mar. 2023.

[15] N. F. J. Waterval, F. Nollet, J. Harlaar, and M.-A. Brehm, “Modifying ankle foot orthosis stiffness in patients with calf muscle weakness: Gait responses on group and individual level,” *Journal of NeuroEngineering and Rehabilitation*, vol. 16, p. 120, Oct. 2019.

[16] N. F. J. Waterval, F. Nollet, J. Harlaar, and M.-A. Brehm, “Precision orthotics: Optimising ankle foot orthoses to improve gait in patients with neuromuscular diseases; protocol of the PROOF-AFO study, a prospective intervention study,” eng, *BMJ open*, vol. 7, no. 2, e013342, Feb. 2017.

[17] H. Ling, H. Guo, H. Zhou, *et al.*, “Effect of a rigid ankle foot orthosis and an ankle foot orthosis with an oil damper plantar flexion resistance on pelvic and thoracic movements of patients with stroke during gait,” *BioMedical Engineering OnLine*, vol. 22, no. 1, p. 9, 2023.

[18] D. van der Wilk, P. U. Dijkstra, K. Postema, G. J. Verkerke, and J. M. Hijmans, “Effects of ankle foot orthoses on body functions and activities in people with floppy paretic ankle muscles: A systematic review,” *Clinical Biomechanics*, vol. 30, no. 10, pp. 1009–1025, Dec. 2015.

[19] V. Creylman, L. Muraru, J. Pallari, H. Vertommen, and L. Peeraer, “Gait assessment during the initial fitting of customized selective laser sintering ankle foot orthoses in subjects with drop foot,” *Prosthetics and Orthotics International*, vol. 37, no. 2, pp. 132–138, 2013.

[20] D. van der Wilk, J. M. Hijmans, K. Postema, and G. J. Verkerke, “A user-centered qualitative study on experiences with ankle-foot orthoses and suggestions for improved design,” EN, *Prosthetics and Orthotics International*, vol. 42, no. 2, pp. 121–128, Apr. 2018.

[21] L. J. Zielstra, I. L. Y. Beck, and N. F. J. Waterval, “Ankle-Foot Orthoses Design Shortcomings: User Complaint Survey,” en, in *Converging Clinical and Engineering Research on Neurorehabilitation V*, J. L. Pons, J. Tornero, and M. Akay, Eds., Cham: Springer Nature Switzerland, 2024, pp. 645–649, ISBN: 978-3-031-77584-0.

[22] *Rezolve Medical | Innovative AFO Solutions*. [Online]. Available: `https://www.rezolvemedical.com/`.

[23] D. Totah, M. Menon, C. Jones-Hershinow, K. Barton, and D. H. Gates, “The impact of ankle-foot orthosis stiffness on gait: A systematic literature review,” *Gait & Posture*, vol. 69, pp. 101–111, Mar. 2019.

[24] N. F. J. Waterval, M. M. van der Krogt, K. Veerkamp, *et al.*, “The interaction between muscle pathophysiology, body mass, walking speed and ankle foot orthosis stiffness on walking energy cost: A predictive simulation study,” en, *Journal of NeuroEngineering and Rehabilitation*, vol. 20, no. 1, p. 117, Sep. 2023.

[25] G. Mathiyazhagan and N. Vasiraja, “Finite element analysis on curved beams of various sections,” in *2013 International Conference on Energy Efficient Technologies for Sustainability*, Apr. 2013, pp. 168–173.

[26] J. Dygut and M. Piwowar, “Torques in the human upper ankle joint level and their importance in conservative and surgical treatment,” en, *Scientific Reports*, vol. 14, no. 1, p. 7525, Mar. 2024.

[27] D. J. J. Bregman, A. Rozumalski, D. Koops, V. de Groot, M. Schwartz, and J. Harlaar, “A new method for evaluating ankle foot orthosis characteristics: BRUCE,” *Gait & Posture*, vol. 30, no. 2, pp. 144–149, Aug. 2009.

[28] R. W. Bohannon and A. Williams Andrews, “Normal walking speed: A descriptive meta-analysis,” *Physiotherapy*, vol. 97, no. 3, pp. 182–189, Sep. 2011.

[29] C. F. Hovorka, G. F. Kogler, Y.-H. Chang, and R. J. Gregor, “Selective orthotic constraint of lower limb movement during walking reveals new insights into neuromuscular adaptation,” English, *Frontiers in Rehabilitation Sciences*, vol. 5, p. 1 354 115, Jun. 2024.

[30] H. J. Hermens, B. Freriks, R. Merletti, *et al.*, “European Recommendations for Surface ElectroMyoGraphy,” en,

[31] C. Schwartz, F.-C. Wang, B. Forthomme, V. Denoël, O. Brüls, and J.-L. Croisier, “Normalizing gastrocnemius muscle EMG signal: An optimal set of maximum voluntary isometric contraction tests for young adults considering reproducibility,” *Gait & Posture*, vol. 82, pp. 196–202, Oct. 2020.

[32] A. M. Burden, M. Trew, and V. Baltzopoulos, “Normalisation of gait EMGs: A re-examination,” *Journal of Electromyography and Kinesiology*, vol. 13, no. 6, pp. 519–532, Dec. 2003.

[33] A. Ghazwan, S. M. Forrest, C. A. Holt, and G. M. Whatling, “Can activities of daily living contribute to EMG normalization for gait analysis?” *PLoS ONE*, vol. 12, no. 4, e0174670, Apr. 2017.

[34] T. C. Pataky, “Generalized *n*-dimensional biomechanical field analysis using statistical parametric mapping,” *Journal of Biomechanics*, vol. 43, no. 10, pp. 1976–1982, Jul. 2010.

[35] R. B. D’Agostino, “Tests for the Normal Distribution,” in *Goodness-of-Fit-Techniques*, Routledge, 1986, ISBN: 978-0-203-75306-4.

[36] M. A. Moosabhoy and S. A. Gard, “Methodology for determining the sensitivity of swing leg toe clearance and leg length to swing leg joint angles during gait,” *Gait & Posture*, vol. 24, no. 4, pp. 493–501, Dec. 2006.

[37] C. H. So, T. O. Siu, K. M. Chan, M. K. Chin, and C. T. Li, “Isokinetic profile of dorsiflexors and plantar flexors of the ankle–a comparative study of élite versus untrained subjects.,” *British Journal of Sports Medicine*, vol. 28, no. 1, pp. 25–30, Mar. 1994.

[38] G. Avdan, S. Onal, and B. K. Smith, “Normalization of EMG Signals: Optimal MVC Positions for the Lower Limb Muscle Groups in Healthy Subjects,” en, *Journal of Medical and Biological Engineering*, vol. 43, no. 2, pp. 195–202, Apr. 2023.

[39] D. Sidebotham and C. J. Barlow, “The winner’s curse: Why large effect sizes in discovery trials always get smaller and often disappear completely,” en, *Anaesthesia*, vol. 79, no. 1, pp. 86–90, 2024.

[40] E. Pourhoseingholi and N. Tafti, “The efficacy of the Novel Hybrid Passive Spring Damper Ankle Foot Orthosis regard to kinetic and kinematic parameters of patients with Multiple Sclerosis: An intervention study,” *Assistive Technology*, 2024.

Appendices

Appendix A.

Supplementary Table 1: Randomisation order of conditions for all included participants.

Participant	1st	2nd	3rd	4th	5th	6th	7th
P1	Baseline	C3	C5	Sham	C2	C4	C1
P4	Baseline	C5	C3	C2	C4	C1	Sham
P5	Baseline	C4	C2	C3	C1	Sham	C5
P6	Baseline	C5	Sham	C3	C1	C2	C4
P7	Baseline	C1	C4	C2	Sham	C5	C3
P8	Baseline	C4	C1	C3	Sham	C2	C5
P10	Baseline	C5	Sham	C3	C4	C2	C1
P11	Baseline	C4	C3	C2	C5	Sham	C1
P12	Baseline	Sham	C3	C1	C5	C4	C2
P13	Baseline	C2	C4	Sham	C5	C1	C3

Appendix B.

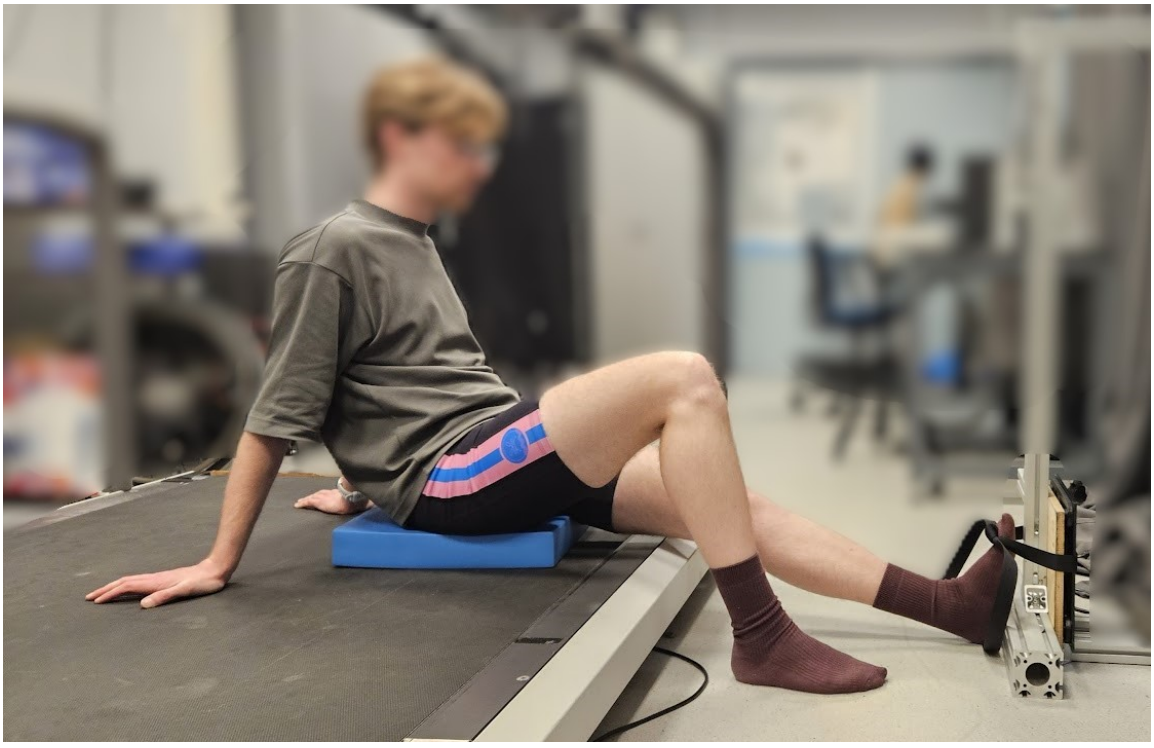

Supplementary Figure 1: Position used for the maximal voluntary isometric contraction test for the tibialis anterior.

Supplementary Figure 2: Position used for the maximal voluntary isometric contraction test for the medial gastrocnemius and soleus.

Appendix C.

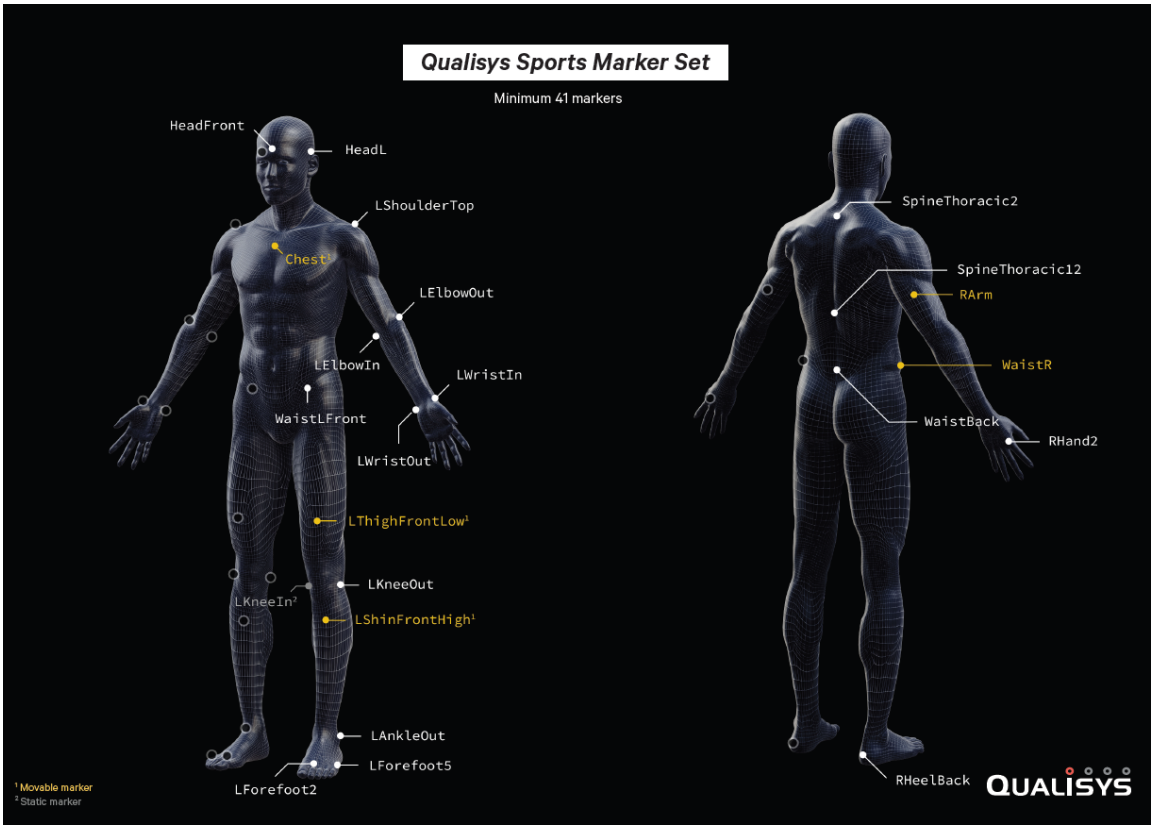

Supplementary Figure 3: Qualisys sports marker set. Only the lower body markers (from the waist down) were used in this research.

Appendix D.

Supplementary Figure 4: Standardised shoes used in the experiment, with motion capture markers that were placed on the shoe instead of on the foot.

Appendix E.

This appendix presents the mechanical design rationale and technical drawings of the interchangeable stiffness modulators used in this study. The stiffness modulator functions as a curved beam, where stress distribution under bending differs from straight beams. In curved beams, stress distribution is asymmetrical with maximum stress occurring in the distal fibres and higher stress concentrations on the inner curve of rectangular cross-sections [25]. To reduce this stress imbalance and prevent failure, the modulator's cross-section was modified from rectangular to trapezoidal, featuring a wider inner curvature and narrower outer side. This design redistributes stress more evenly across the beam during bending. To maintain consistent proportions, the central width of each modulator's cross-section was designed to match its thickness. The technical drawing below shows first an isometric view of stiffness modulator C3, followed by a side profile of all stiffness modulators used in this study, with their cross-sections shown below. Dimensions are in mm.

Technical drawing
Interchangeable stiffness modulator

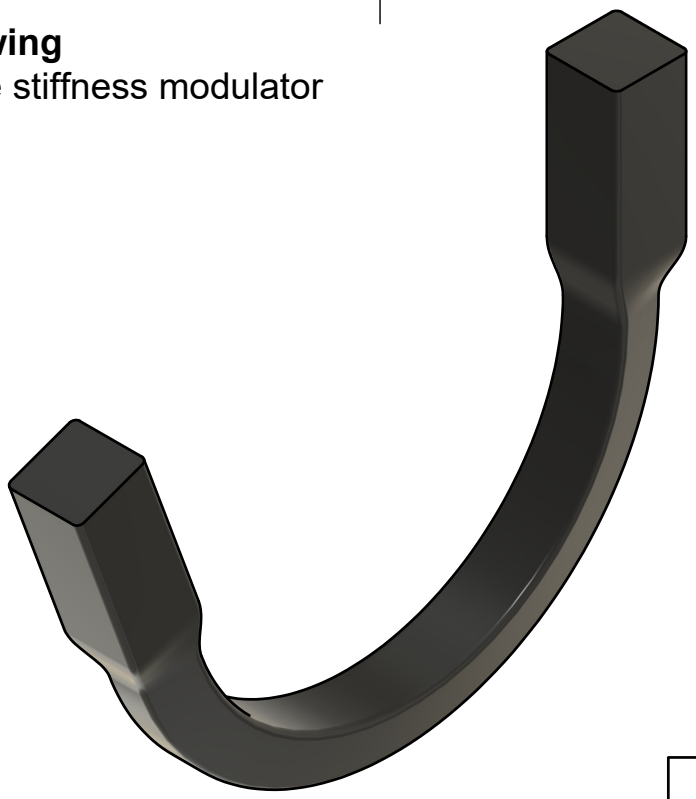

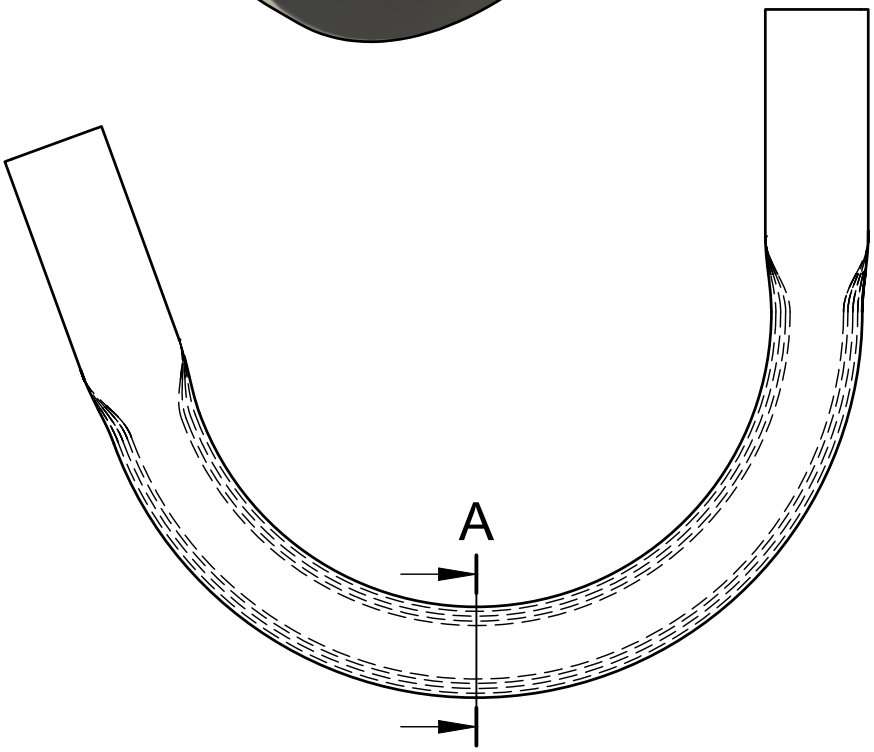

A-A (1:1)

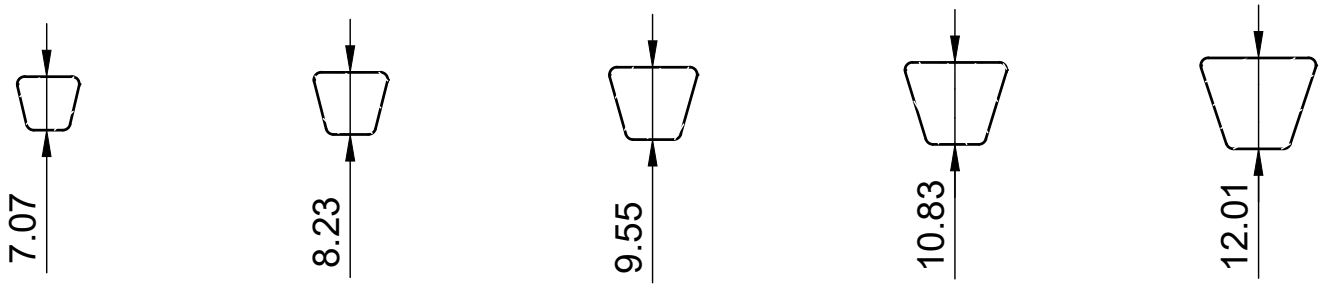

Appendix F.

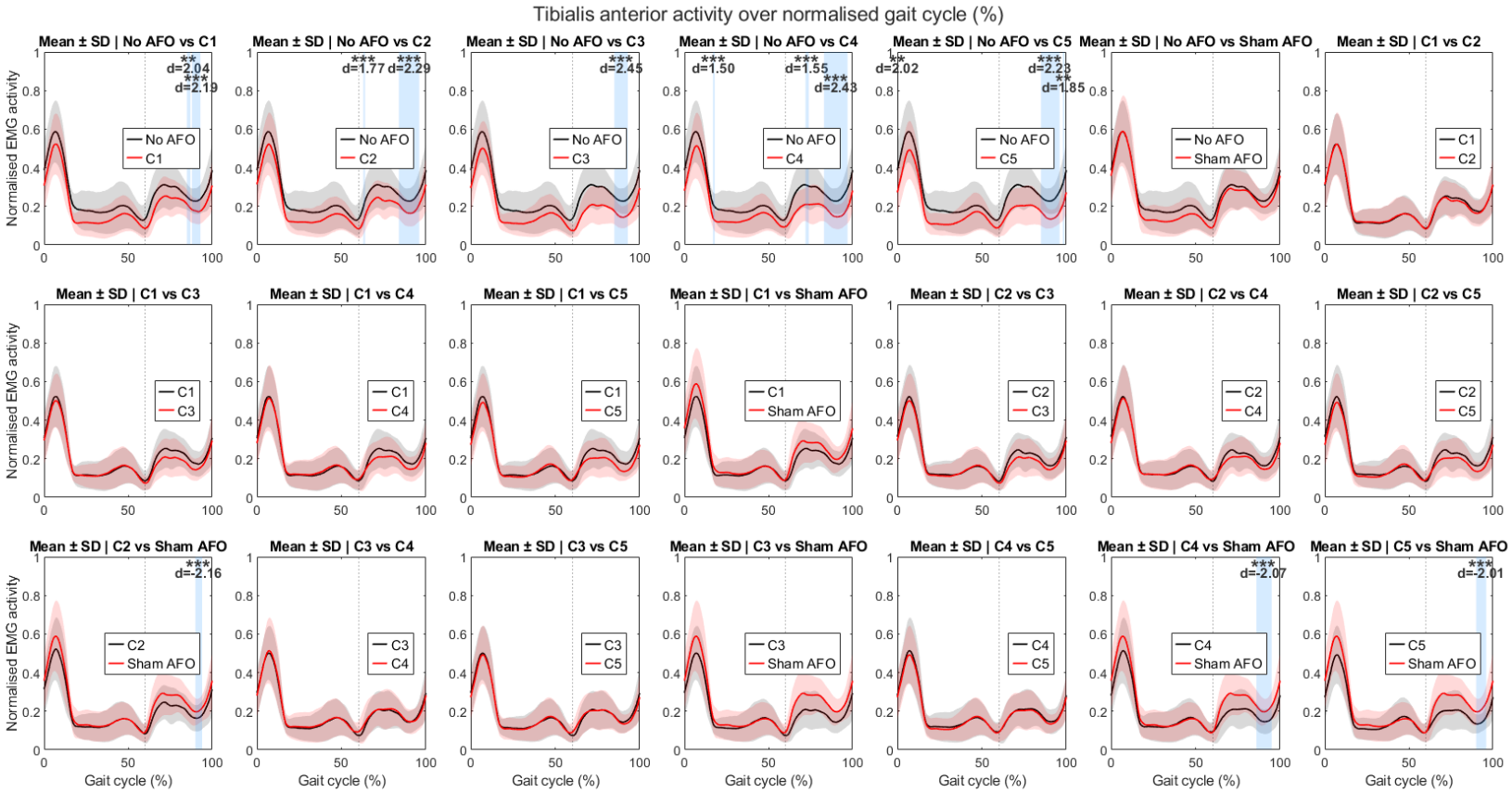

Supplementary Figure 5: Average normalised tibialis anterior EMG activity across all participants over the gait cycle, with standard deviation represented by shaded areas. Each subplot shows a pairwise comparison between conditions, including the baseline (no AFO), all Rise AFO configurations (C1–C5), and the sham AFO. Statistically significant differences identified by SPM are highlighted in blue, with significance levels indicated (*p ≤ 0.05, **p ≤ 0.01, ***p ≤ 0.001) and corresponding effect sizes (Cohen's d) shown above. The x-axis denotes the normalised gait cycle (0–100%), and the y-axis normalised muscle activity. The vertical line at 60% marks the transition from stance to swing phase.

Appendix G.

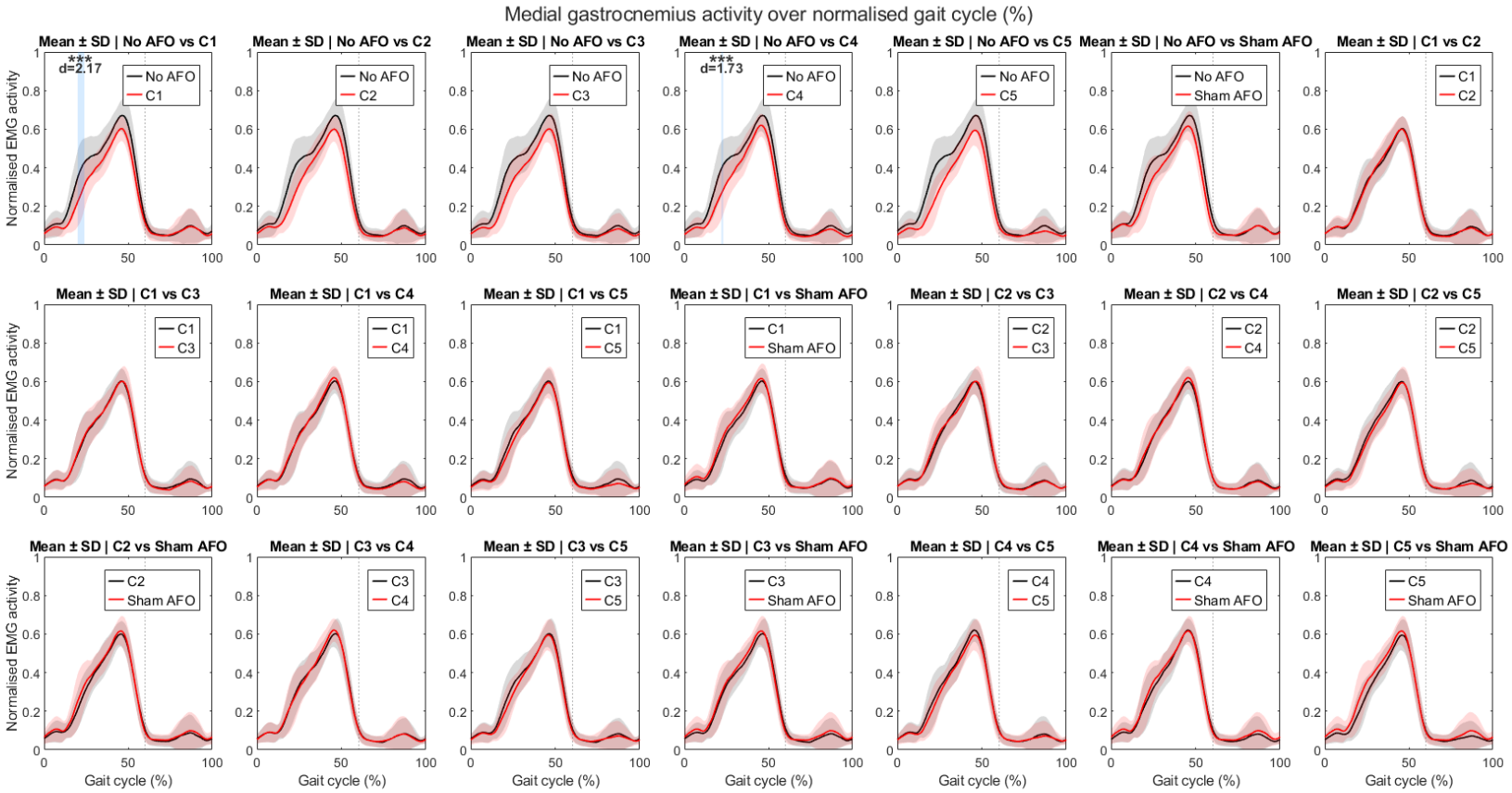

Supplementary Figure 6: Average normalised medial gastrocnemius EMG activity across all participants over the gait cycle, with standard deviation represented by shaded areas. Each subplot shows a pairwise comparison between conditions, including the baseline (no AFO), all Rise AFO configurations (C1–C5), and the sham AFO. Statistically significant differences identified by SPM are highlighted in blue, with significance levels indicated (*p ≤ 0.05, **p ≤ 0.01, ***p ≤ 0.001) and corresponding effect sizes (Cohen's d) shown above. The x-axis denotes the normalised gait cycle (0–100%), and the y-axis normalised muscle activity. The vertical line at 60% marks the transition from stance to swing phase.

Appendix H.

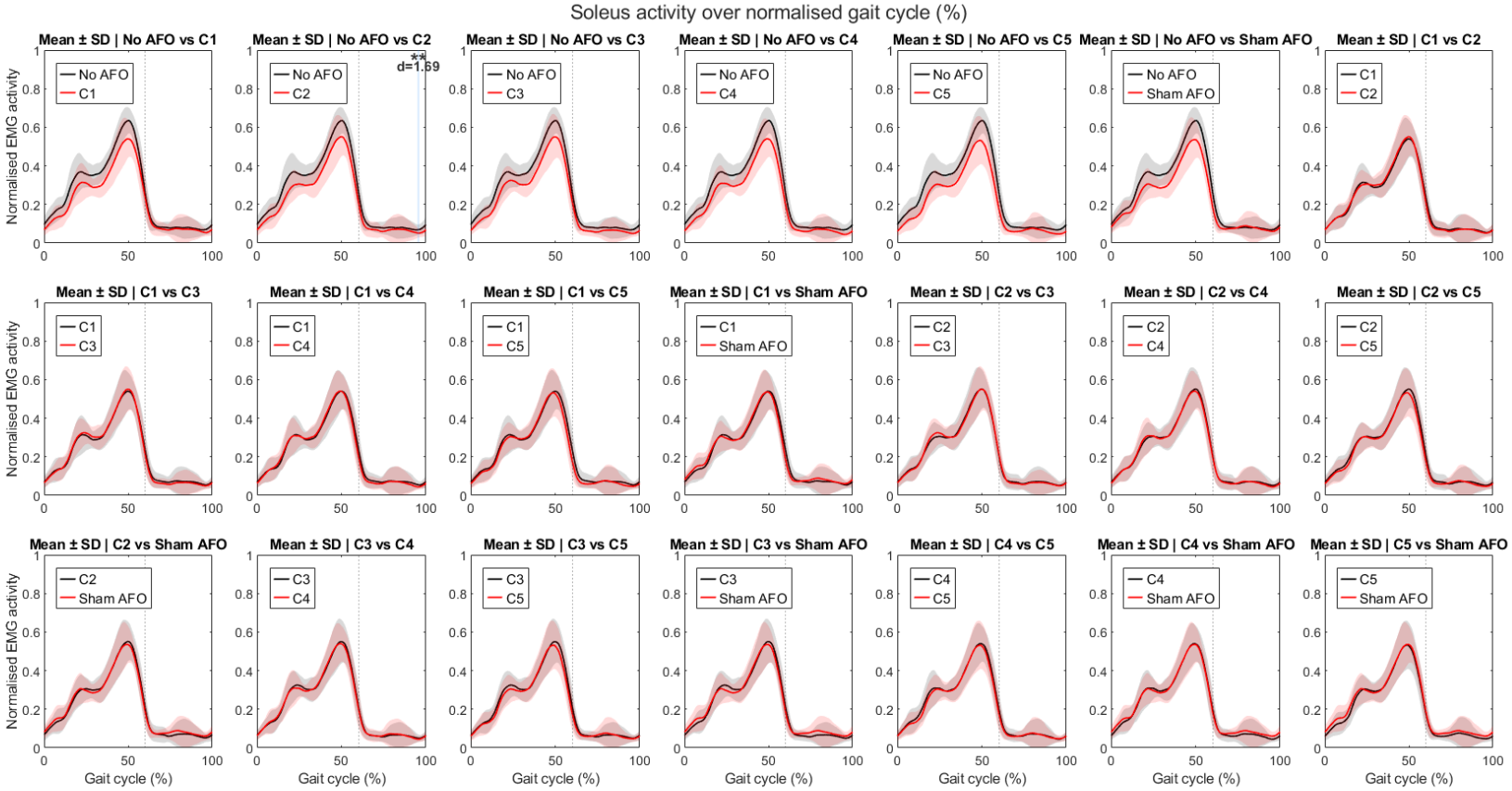

Supplementary Figure 7: Average normalised soleus EMG activity across all participants over the gait cycle, with standard deviation represented by shaded areas. Each subplot shows a pairwise comparison between conditions, including the baseline (no AFO), all Rise AFO configurations (C1–C5), and the sham AFO. Statistically significant differences identified by SPM are highlighted in blue, with significance levels indicated (*p ≤ 0.05, **p ≤ 0.01, ***p ≤ 0.001) and corresponding effect sizes (Cohen's d) shown above. The x-axis denotes the normalised gait cycle (0–100%), and the y-axis normalised muscle activity. The vertical line at 60% marks the transition from stance to swing phase.

Appendix I.

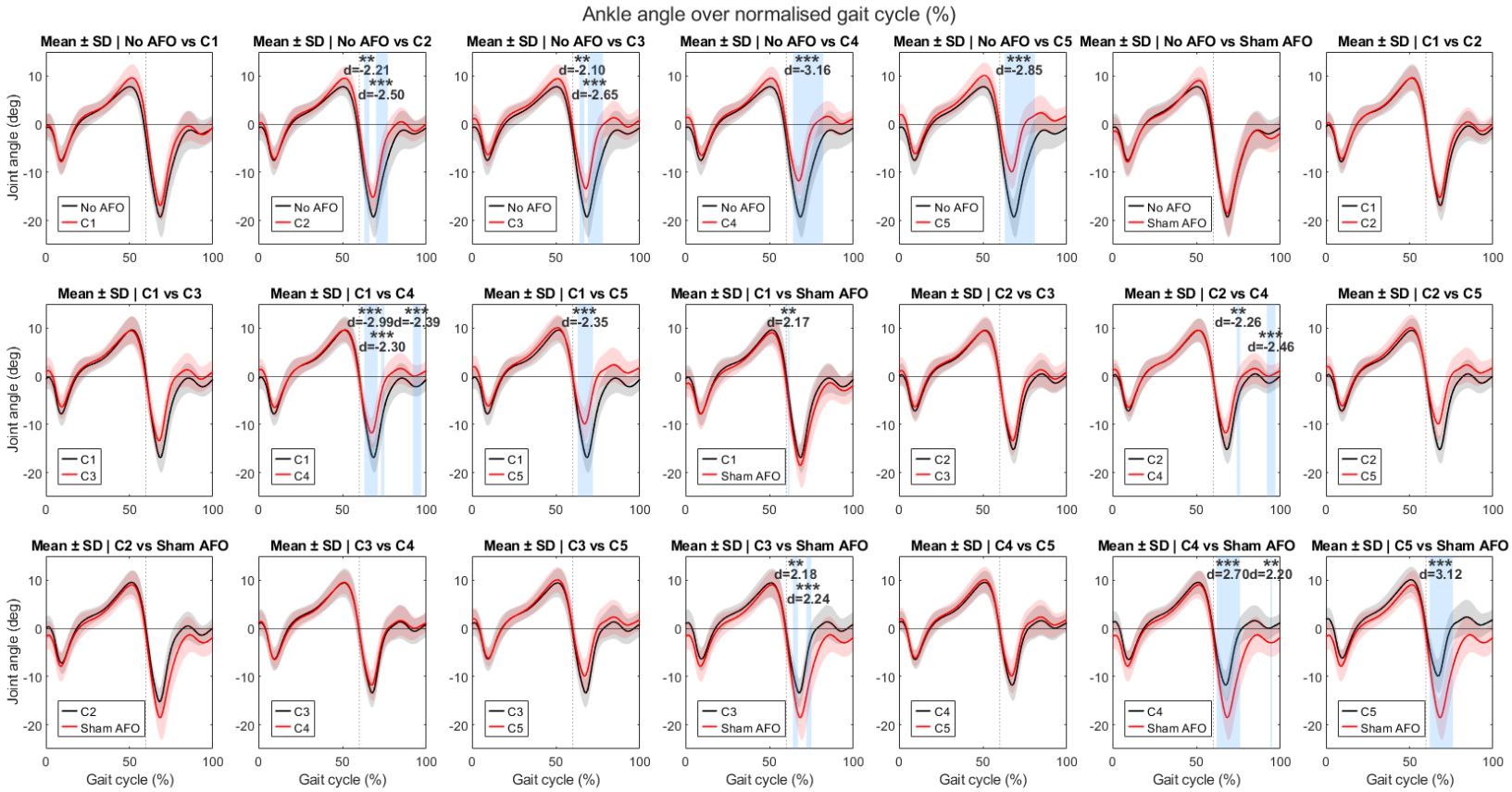

Supplementary Figure 8: Average ankle flexion across all participants over the gait cycle, with standard deviation represented by shaded areas. Each subplot shows a pairwise comparison between conditions, including the baseline (no AFO), all Rise AFO configurations (C1–C5), and the sham AFO. Statistically significant differences identified by SPM are highlighted in blue, with significance levels indicated (*p ≤ 0.05, **p ≤ 0.01, ***p ≤ 0.001) and corresponding effect sizes (Cohen's d) shown above. The x-axis denotes the normalised gait cycle (0–100%), and the y-axis ankle flexion, with dorsiflexion defined as positive and plantarflexion as negative. The vertical line at 60% marks the transition from stance to swing phase.

Appendix J.

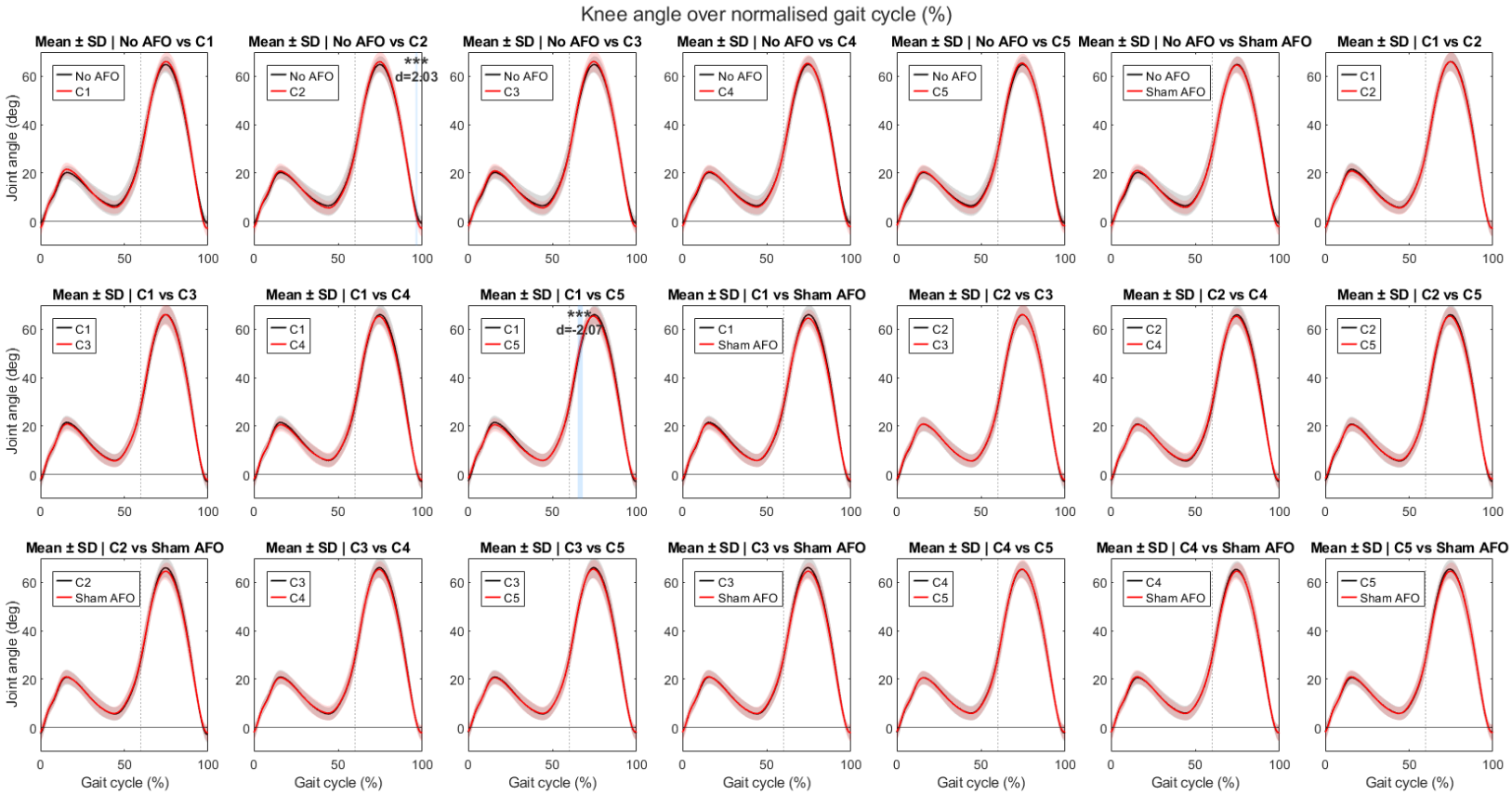

Supplementary Figure 9: Average knee flexion across all participants over the gait cycle, with standard deviation represented by shaded areas. Each subplot shows a pairwise comparison between conditions, including the baseline (no AFO), all Rise AFO configurations (C1–C5), and the sham AFO. Statistically significant differences identified by SPM are highlighted in blue, with significance levels indicated (*p ≤ 0.05, **p ≤ 0.01, ***p ≤ 0.001) and corresponding effect sizes (Cohen's d) shown above. The x-axis denotes the normalised gait cycle (0–100%), and the y-axis ankle flexion, with flexion defined as positive and extension as negative. The vertical line at 60% marks the transition from stance to swing phase.

Appendix K.

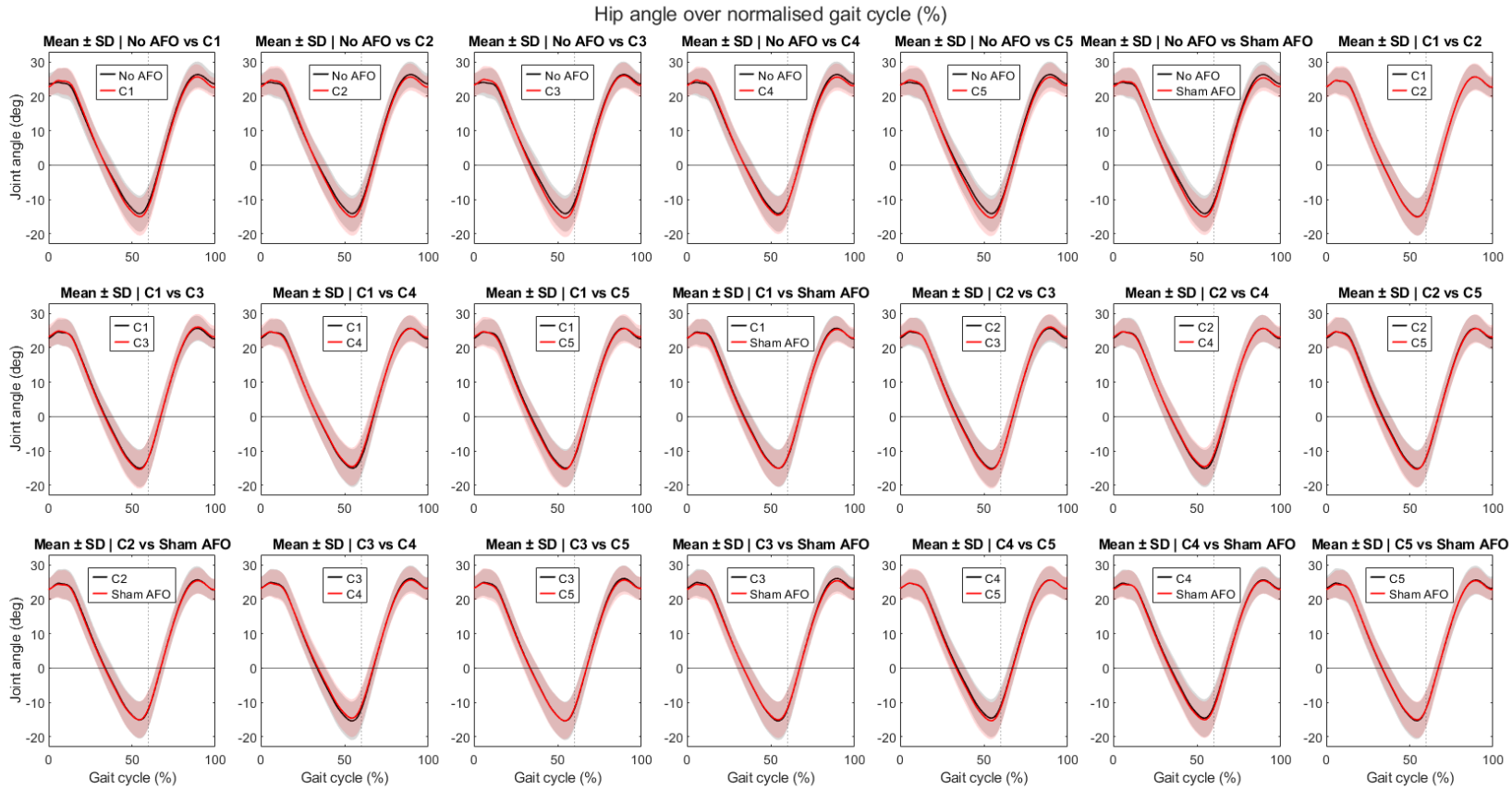

Supplementary Figure 10: Average hip flexion across all participants over the gait cycle, with standard deviation represented by shaded areas. Each subplot shows a pairwise comparison between conditions, including the baseline (no AFO), all Rise AFO configurations (C1–C5), and the sham AFO. Statistically significant differences identified by SPM are highlighted in blue, with significance levels indicated (*p ≤ 0.05, **p ≤ 0.01, ***p ≤ 0.001) and corresponding effect sizes (Cohen's d) shown above. The x-axis denotes the normalised gait cycle (0–100%), and the y-axis ankle flexion, with flexion defined as positive and extension as negative. The vertical line at 60% marks the transition from stance to swing phase.